Available online at www.sciencedirect.com
ScienceDirect
Polymer 48 (2007) 5473–5479
polymer
www.elsevier.com/locate/polymer

Polymer Communication

Potential controlled electrochemical assembly of chiral polyaniline with enhanced stereochemical selectivity

Xuetong Zhang [a,b,*], Wenhui Song [b]

[a] School of Chemistry, University of York, Heslington, York YO10 5DD, UK
[b] Wolfson Center for Materials Processing, School of Engineering and Design, Brunel University, West London UB8 3PH, UK

Received 24 May 2007; received in revised form 15 July 2007; accepted 19 July 2007
Available online 26 July 2007

Abstract

Chiral polyaniline with absolute sterochemical selectivity in the order of magnitude 10^{-2} is electrochemically assembled onto various electrodes in the presence of chiral inducing agent (1*S*)-(+)-10-camphorsulfonic acid ((*S*)-(+)-CSA) or (1*R*)-(−)-10-camphorsulfonic acid ((*R*)-(−)-CSA). The polymerizing potential dependence of the absolute stereochemical selectivity of the resultant chiral polyaniline is investigated in detail. The one-step (low potential at 0.7 V) and two-step (potential higher than that of aniline oxidation potential of the electrode applied first in the short period of time and then low potential at 0.7 V applied in the relatively long time) potential control strategies are developed for the different conducting substrates in order to produce chiral polyaniline with enhanced absolute stereochemical selectivity. The possible mechanism on polymerizing potential dependence of chiral polyaniline with enhanced absolute stereochemical selectivity is discussed. The structure and morphology of the resultant polyaniline films are investigated by scanning electron microscopy (SEM). The strong mirror images of the circular dichroism (CD) spectra for the (*R*)-(−)-CSA and the (*S*)-(+)-CSA doped polyaniline films suggest that the obtained chiral polyaniline films are enantioselective.

Keywords: Conducting polymers; Chirality; Electrochemical deposition

1. Introduction

Chiral structures are often observed in biomacromolecules and play a dominant role in living systems, as exemplified by protein and DNA, which adopt a right-handed R-helix and a double helix, respectively [1,2]. In the past decade there has been increasing interest in synthesizing chiral conducting polymers due to their potential applications in circular polarized electroluminescence device, chemical and biochemical sensor, surface-modified electrode, chiral separation, chiral recognition, etc. [3–9]. Among the conducting polymers, chiral polyaniline has attracted considerable attention because it is inexpensive, easily synthesized, and environmentally stable. Covalent attachment of a chiral substitute to amine nitrogen centers on aniline repeat units, was a seldom-used strategy for chiral polyaniline (derivatives) due to the time consuming and expensive production of the chiral monomers [10]. Actually the first preparation of chiral polyaniline from the achiral monomers was reported as early as in 1994 [11,12] and the approach involved in situ enantioselective (electro-) polymerization of aniline in the presence of an optically active acid as a chiral inducing agent. So far this method has been popular in preparing the chiral polyaniline [13,14] and even successfully applied to synthesize optically active colloids [15] and nanostructures [16] of the polymer. A chiral acid ex situ doping of preformed emeraldine base of the polyaniline in an organic solvent was also applied to cast chiral films based on reversible doping [17,18].

However, most of the chiral polyaniline synthesized from the above methods suffer from low absolute stereochemical selectivity. Recently Wang and Li have reported the synthesis of the chiral polyaniline with anisotropy factor ($g = \Delta\varepsilon/\varepsilon$) as

* Corresponding author. School of Chemistry, University of York, Heslington, York YO10 5DD, UK. Tel.: +44 1904 432544; fax: +44 1904 432516.
E-mail address: xz523@york.ac.uk (X. Zhang).

0032-3861/$ - see front matter © 2007 Elsevier Ltd. All rights reserved.
doi:10.1016/j.polymer.2007.07.044

high as 2.3×10^{-2} via solution chemistry and electrochemistry [19,20], respectively. In comparison with other approaches, the most striking difference is that oligomer was used for accelerating the polymerization reaction in the presence of the highly concentrated chiral inducing agent. By applying this method, we have successfully synthesized chiral polyaniline/carbon nanotube nanocomposites with desirable absolute stereochemical selectivity [21,22]. Although it is a feasible method in synthesizing the chiral polyaniline (even its composites) so far with highest absolute stereochemical selectivity, there are some disadvantages existing: (1) the absolute stereochemical selectivity of the resultant chiral polyaniline is greatly dependent on the oligomer used, and (2) some commercially unavailable oligomers need extra time and cost to be synthesized for use.

In this study, a facile electrochemical assembly of the chiral polyaniline with enhanced absolute stereochemical selectivity is reported. The chiral polyaniline films can be electrodeposited onto general conducting substrates from metal (gold, Au), metal oxide (indium tin oxide, ITO) to nonmetal (graphite, C), respectively, by simply controlling the potential in the presence of a chiral inducing agent (1*S*)-(+)-10-camporsulfonic acid ((*S*)-(+)-CSA) or (1*R*)-(−)-10-camporsulfonic acid ((*R*)-(−)-CSA). Although no oligomers are used during electrodeposition, the resultant chiral polyaniline is with the anisotropy factor up to 2.0×10^{-2}, comparable to that reported by Wang and Li [19,20].

2. Experimental section

2.1. Materials

All chemicals were purchased from Sigma–Aldrich Company Ltd. Aniline was purified by distillation before use. Other reagents were used as received without further purification.

2.2. Electrochemical deposition

All the electrochemical experiments were carried out at room temperature in a one-compartment cell by using the IM6 Electrochemical Workstation and all potentials were referred to a saturated calomel electrode (SCE). All electrodes were cleaned before use, including working electrodes [gold on silicon chip from Structure Probe Inc., USA; indium tin oxide (ITO) coated glass slide from Sigma–Aldrich Company Ltd.; and carbon rod from Fisher Scientific. Co. Ltd.] and counter electrode (Pt wire from Sigma–Aldrich Company Ltd.). The electrolyte was a mixture of 7.5 mL H_2O, 0.66 mL aniline and 12.0 g (*S*)-(+)-/(*R*)-(−)-CSA. After electrodeposition, the resultant films were flushed with deionized water and methanol in sequence and then dried for morphology observation. The fresh and clean electrodeposited films were also peeled off into the water by sonication for spectroscopy investigation.

2.3. Instrumentation

The morphology of the resulting films was characterized using ZEISS Supra 35 field-emission-gun scanning electron microscope (FEGSEM) at 5–10 kV. UV and CD spectra were acquired on the JASCO J720 spectropolarimeter, calibrated with a reference standard (ammonium d-10-camphor sulphonate) JASCO Standard prior to the actual experiments. All the spectra were recorded in 780–200 nm using a 10 mm rectangular cell path-length. The sample was placed as near as possible to the instrument detector to minimize light scattering effects. The following parameters were used: 2 nm bandwidth, 20 nm min^{-1} speed, 4 s time constant and 1 nm step-size. All spectra were solvent baseline subtracted and acquired at room temperature. All the CD spectra were normalized according to UV absorbance $A_{440\,nm} = 1.0$ in this study.

3. Results and discussion

To clarify how to control the potential during the electrodeposition, the potential (vs. SCE) dependence of the aniline electropolymerization is to be understood in the first instance. Fig. 1a shows the first forward scans respectively of using gold, ITO and graphite as working electrodes recorded at 50 mV s^{-1} in the aqueous electrolyte containing aniline and CSA. It can be seen that the aniline polymerization onto the different electrodes initiates with the different oxidation potentials. In comparison with the Au electrode (its aniline oxidation potential is ca. 0.9 V), the graphite electrode starts with the lower oxidation potential (ca. 0.8 V) while the ITO electrode starts with the higher oxidation potential (ca. 1.0 V) for the aniline electropolymerization. The difference in the initiation oxidation potentials of the aniline onto the different electrodes ascribes to structural nature and surface properties of the electrode materials [22]. While Fig. 1b shows the cyclic voltammogram scans using gold as working electrode recorded at the same scanning rate in the same electrolyte as shown in Fig. 1a. As shown in Fig. 1b, redox peaks (b) indicate conversion of emeraldine to pernigraniline and the peak (a)/(a′) corresponds to the redox of dimers and/or the benzoquinone/hydroquinone couple [23]. It is obvious that the aniline oxidation potential decreases gradually with the increase of the scan times: originally the aniline electropolymerization initiates at the potential ca. 0.9 V while after four times of the cyclic voltammogram scans the aniline electrodeposition occurs at the potential between 0.6 and 0.7 V. These dynamic chain-initiation potentials shift towards the low potential direction with the increase of the scan cycles, known as autocatalysis phenomenon [24], and is also observed by using graphite or ITO as the working electrode in our experiments. The aniline autocatalysis electropolymerization results from the oligomers produced in situ during scans with the oxidation potential lower than that of the aniline [20]. The larger the molecular weight of the oligomer, the lower the oxidation potential [20].

To investigate polymerizing potential dependence of the obtained optical activity of the polyaniline, we have applied the different constant potentials for electrochemical assembly of the aniline onto the Au electrode. In comparison with the aniline oxidation potential (ca. 0.9 V for this case as shown in Fig. 1a), when higher potential (e.g. 0.95 V) is applied, the electropolymerization of the aniline almost occurs

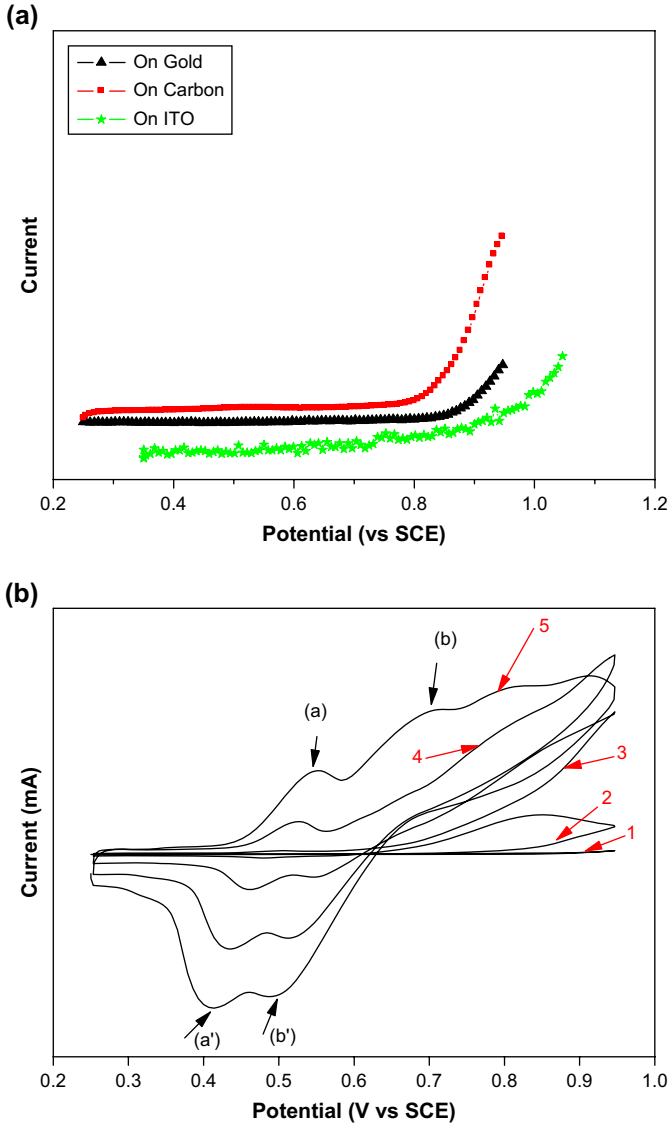

Fig. 1. (a) First forward potential dynamic scanning curves using graphite, gold and indium tin oxide as working electrodes, respectively, and (b) typical cyclic voltammogram scanning curves using gold as working electrode. (In all cases the electrolyte was a mixture of 7.5 mL H_2O, 0.66 mL aniline and 12.0 g (*S*)-(+)-/(*R*)-(−)-CSA.).

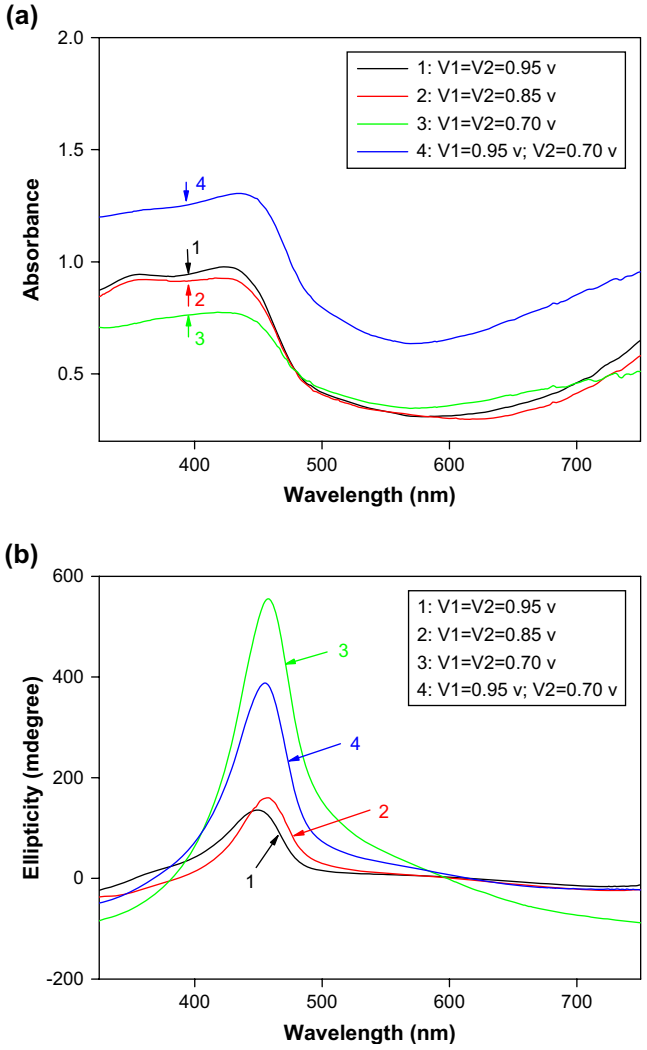

Fig. 2. UV (a) and normalized CD (b) spectra of the chiral polyaniline electrodeposited onto the Au electrode at the different potentials (curve 1−3 recorded from the polyaniline electrodeposited by one-step potential ($V = 0.95$, 0.85, and 0.70 V, respectively) and curve 4 recorded from the polyaniline electrodeposited by two-step potential ($V_1 = 0.95$ V lasted 40 s and then $V_2 = 0.70$ V) lasted long enough for desirable thickness of the film).

immediately. However, when lower potential (e.g. 0.85 or 0.70 V) is applied, there is an evident incubation period of time before the electropolymerization. The lower the potential applied, the longer the period of the incubation. It has been rationalized that oligomers are produced slowly in this period [20] and thus the aniline can be polymerized with the oligomers due to their lower oxidation potentials. While simultaneous UV absorbance and CD spectra were measured according to the principles described by Drake et al. [25] with the anisotropy *g*-factor defined as the ratio CD/(absorbance × 32,980). All the polyaniline deposited by applying the different constant potentials show the similar UV spectra as shown in Fig. 2a: peaks at 355 and 440 nm and the long tail started from 600 nm correspond to transition from the π to π* band, localized polaron to π* band, and the π to polaron band [17], respectively. These spectroscopic features are characteristic of the emeraldine salt of the polyaniline, which proves that the chiral inducing agent CSA is doped into the polymer backbone. However, the effect of applied potentials on the stereochemical selectivity of the polymer is significant as shown in Fig. 2b: the polyaniline deposited at the potential as low as 0.7 V shows strongest CD intensity with the *g*-factor as high as 1.8×10^{-2}, while the polyaniline deposited at potential range 0.95−0.70 V shows the increase of the CD intensity with the decrease of the potential. When (*R*)-(−)-CSA is used, all the polyaniline deposited at the constant potential gave a peak around 457 nm with a positive Cotton effect although there is a small blue shift for polyaniline electrodeposited at 0.95 V. It is concluded that the asymmetrical (helical) conformation and/or chain-packing are mostly responsible for its optical activity (stereochemical selectivity) when using CSA as a chiral inducing agent for the synthesis of chiral polyaniline [19,20] as CSA itself gives a strong peak at 290 nm. These facts have

illustrated that the potential as low as 0.7 V favors the helical conformation or chain-packing of the polymer.

Although the underlying mechanism concerning how the electro-polymerizing potentials influence the absolute setereochemical selectivity of the polyaniline is not clearly understood, we hypothesize that there is a ''rate match'' between the chain propagation and helical conformation (or chain-packing) in chiral polyaniline assembly. The rate of the helical conformation should be potential independent, however, specific electrostatic and hydrogen bonding between the polyaniline chain and the enantiomeric dopant CSA^- anions are significant for the polymer to preferentially adopt a helical screw [13]. Therefore the rate of the helical conformation of the polyaniline is greatly dependent on the concentration of the chiral inducing agent CSA. We have kept the electrolyte with the same concentration of the CSA in our experiments and thus the rate of the helical conformation does not change all the time. On the other hand, the rate of the chain propagation is very dependent on the potentials as the polymerization current increases with the increase of the polymerizing potential. During the electrodeposition, only potential at 0.7 V gives the most matchable rates between the chain propagation and helical conformation, so the chiral polyaniline with the highest absolute stereochemcial selectivity is observed, Fig. 2b. When the polymerizing potentials are higher (e.g. 0.85 or 0.95 V), there is a rate mismatch as the rate of the chain propagation is faster than that of the helical conformation and accordingly the polyaniline shows lower optical activity. That is why there is a significant difference in optical activity for chiral polyaniline electroposited at 0.85 and 0.70 V, both below the aniline oxidation potentials (0.9 V as shown in Fig. 1) with a period of incubation. When potential is lower than 0.7 V, the incubation period is too long to initiate the polymerization of aniline onto the surface of the Au electrode.

Fig. 3 shows SEM images of the electrodeposited polyaniline films onto the Au electrode by applying the different potentials. It can be clearly seen that the morphology of the resultant chiral polyaniline films is greatly dependent on the polymerizing potential. When high potential (e.g. 0.95 V) is applied, the bulk film is obtained as shown in Fig. 3a. However, when low potential (e.g. 0.70 V) is applied, the film with fiber-like nanostructures twisted and tangled together is observed as shown in Fig. 3b. Such a morphology difference is introduced by the different polymerization rates when applying the different polymerizing potentials. When 0.95 V is applied, which is higher than that of aniline oxidation potential (0.9 V), the polymerization probabilities of all the aniline diffused onto the surface of the Au electrode are the same. This means that there is no preference for polyaniline film to grow along a specific direction or space. So the bulk film of the chiral polyaniline will be observed. However, when 0.70 V is applied, there is a long period of incubation for aniline polymerization as the potential applied is quite lower than that of aniline oxidation potential (0.9 V) and the oligomer is produced during the period of incubation. Once oligomer is formed, due to lower oxidation potential of the oligomer, the aniline will polymerize with the oligomer. This means that there is a preference for polyaniline film to grow along the location of the oligomer. So the nanofibrous film of the chiral polyaniline will be observed.

Respective electrodeposition of chiral polyaniline onto the graphite and ITO electrodes is also investigated by applying the different constant potentials. When the graphite is used as the working electrode, the resultant chiral polyaniline shows similar polymerizing potential dependence of absolute stereochemical selectivity as that of the polyaniline electrodeposited by using Au as the working electrode as shown in Fig. 4. The anisotropy g-factor of the chiral polyaniline is up to 2.0×10^{-2} when 0.70 V constant potential is applied. However, when 0.7 V is applied onto the ITO electrode, no obvious chiral polyaniline is observed as the period of incubation is too long to initiate the polymerization of the aniline. It can be seen from Fig. 1a that the aniline oxidation potentials onto the graphite, Au and ITO electrodes are 0.8, 0.9 and 1.0 V, respectively. We have stated above that, when potential lower than aniline oxidation potential is applied, there is an evident incubation period of time before the electropolymerization. The lower the potential applied, the longer the period of the incubation. If all the electrodes applied constant potential at 0.7 V, obviously there is relatively the lowest potential applied onto the ITO among these electrodes in comparison with their respective aniline oxidation potentials, which results in the longest period of incubation for ITO electrode. This is the reason why chiral polyaniline can be electropolymerized onto the

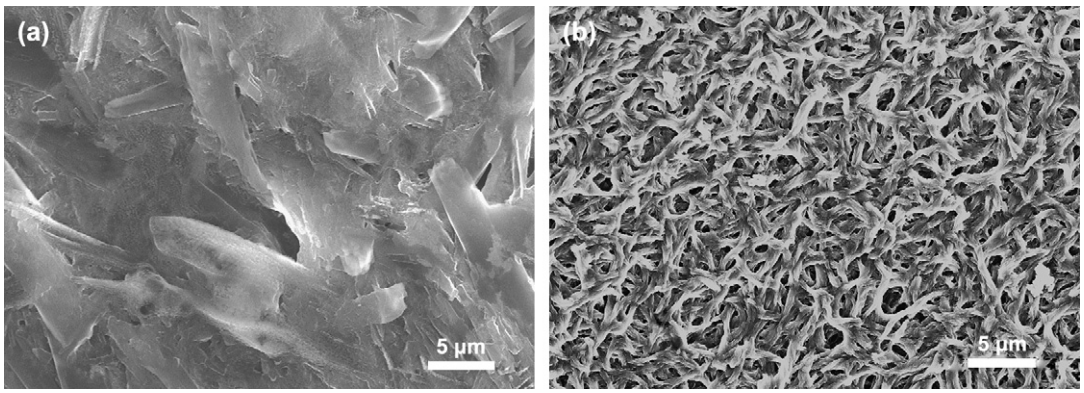

Fig. 3. SEM images of the electrodeposited chiral polyaniline films onto the Au electrode by applying the different potential: 0.95 V (a) and 0.70 V (b).

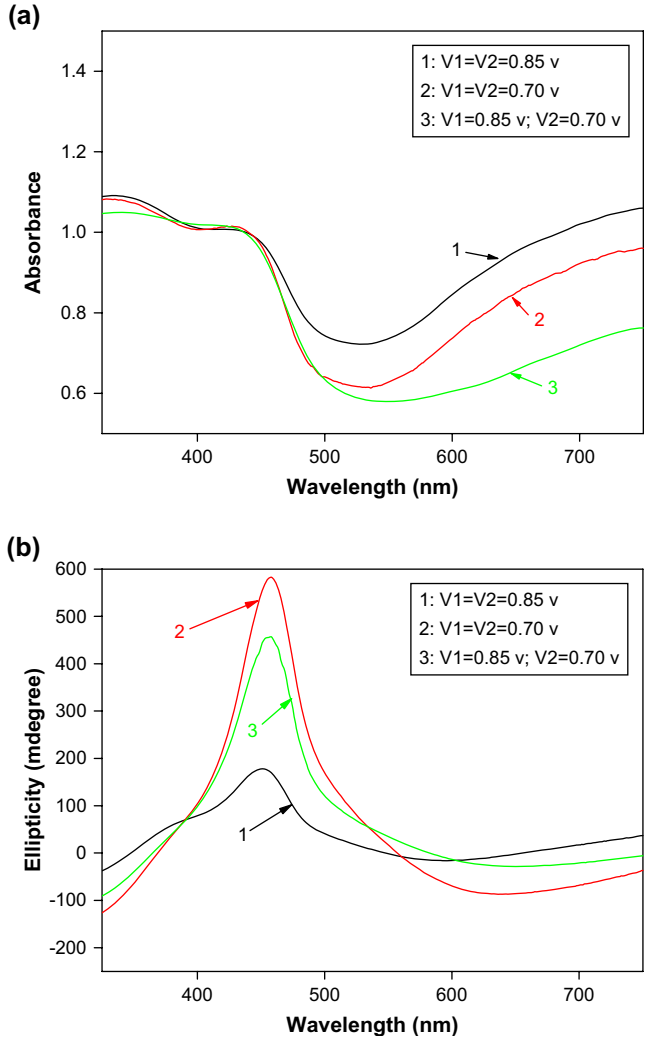

Fig. 4. Normalized UV (a) and CD (b) spectra of the chiral polyaniline electrodeposited by applying different potentials onto graphite electrode.

graphite and Au electrodes rather than ITO electrode by applying the same constant potential at 0.7 V.

In order to shorten or remove the period of incubation in the electrodeposition of chiral polyaniline onto some passivated electrodes such as ITO with the high aniline oxidation potentials, a two-step potential control strategy is developed (constant potential control means one-step manner). For example, during the electrodeposition of the chiral polyaniline onto the Au electrode, the potential is first applied at 0.95 V for a very short period of time (tens of seconds) and then at 0.70 V for a period of time up to obtaining the film with desirable thickness. The resultant chiral polyaniline shows the satisfactory stereochemical selectivity, which is quite higher than that of polyaniline electrodeposited at the potential 0.85–0.95 V while a little lower than that of polyaniline electroposited at 0.70 V as shown in Fig. 2.

For different working electrodes, on applying the two-step potential strategy the second potentials control the same at 0.70 V, while the first potentials are different: 0.85 V for graphite, 0.95 V for Au and 1.05 V for ITO. All the controlled first potential values are a little higher than their respective aniline oxidation potentials. By applying this two-step potential strategy, the chiral polyaniline with desirable stereochemical selectivity is, respectively, electrodeposited onto the graphite, Au and ITO electrodes as shown in Fig. 5. The strong mirror image of the CD spectra for the (*R*)-(−)-CSA and the (*S*)-(+)-CSA doped polyaniline films suggests that our electrochemical assembly of the chiral polyaniline films is enantioselective. The similarity of the UV and CD peak position indicates that the nature of the electrode materials does not strongly affect the aniline polymerization once initiated. However, the absolute stereoselectivity corresponding to the CD peak intensity of the chiral polyaniline varies depending on the electrode materials. A descending order of the electrode materials, sorted by the stereochemical selectivity of the corresponding polyaniline films, is C > Au > ITO.

Fig. 6 shows the typical structure and morphology of the chiral polyaniline film electrodeposited onto the Au electrode by applying the two-step potential. The SEM images in

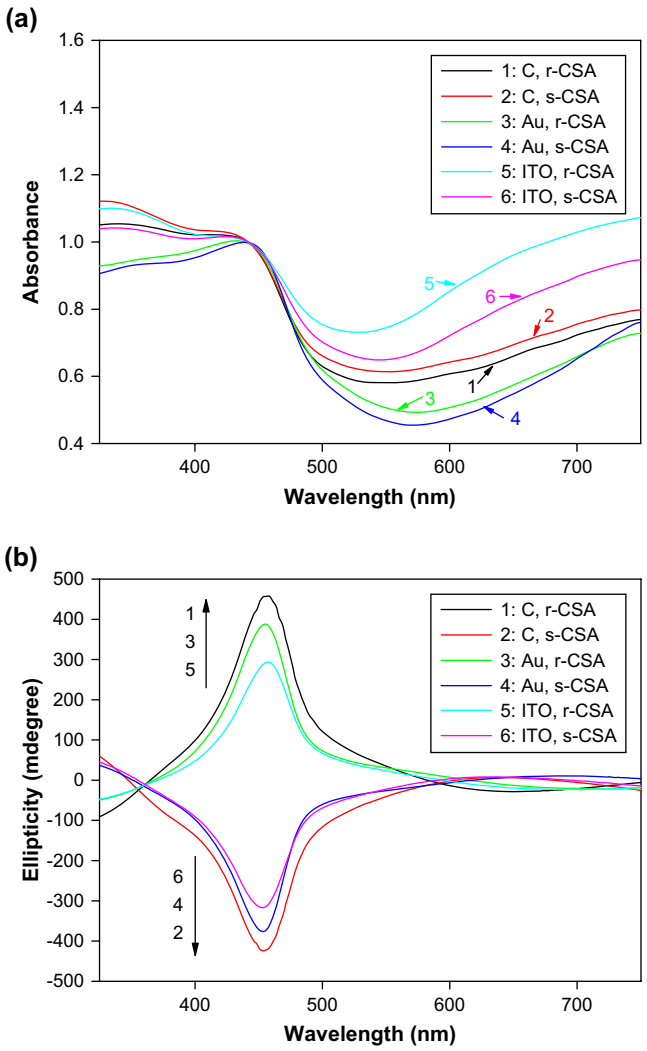

Fig. 5. Normalized UV (a) and CD (b) spectra of the chiral polyaniline electrodeposited by applying two-step potentials onto the different electrodes.

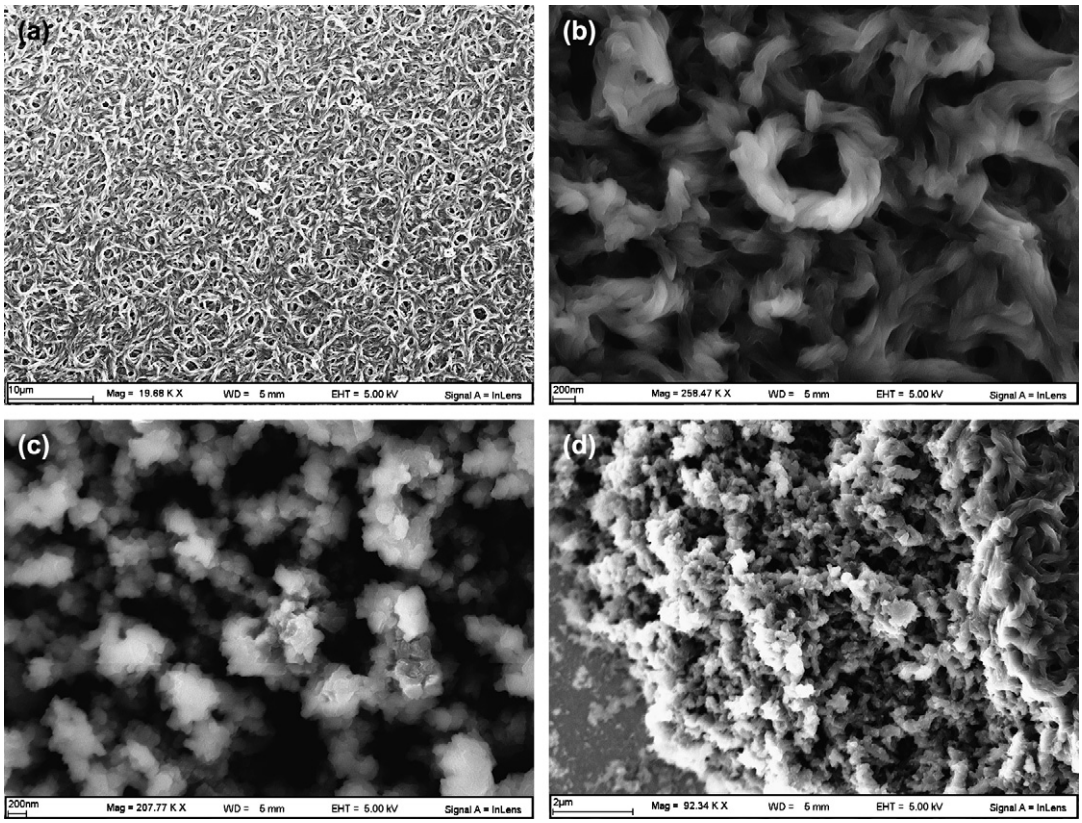

Fig. 6. SEM images of the chiral polyaniline electrodeposited onto Au electrode by applying two-step potential: (a) and (b) top surface; (c) bottom surface and (d) cross-section.

Fig. 6a, b and d reveal that fibrous structures, with the dimension of 10 s of nanometers similar to the structure previous reported for chiral polyaniline nanofibers [20], twist and tangle into a random porous mat. The SEM image in Fig. 6c reveals that the fibrous structures start to grow from separated ''islands'', which is created by applying the first potential in the very short period of time. When Au electrode is replaced by graphite or ITO electrode, the similar structure of the polyaniline film remains. The structure and morphology of the chiral polyaniline films obtained by applying the two-step potential are very similar as that of the chiral polyaniline film obtained by applying the one-step potential at 0.7 V onto various conducting substrates, only if the chiral polyaniline film can be obtained onto the electrode by applying the potential at 0.7 V.

4. Conclusions

In summary, a facile and generic electrochemical method for the chiral polyaniline assembly onto various conducting substrates is demonstrated. By controlling the potential in one-step (low potential at 0.7 V) or two-step (potential higher than that of aniline oxidation potential of the electrodes applied first in the short period of time and then low potential at 0.7 V applied in the relatively long time), the resultant chiral polyaniline shows the enhanced absolute stereochemical selectivity with the anisotropy g-factor up to 2.0×10^{-2}. These chiral polyaniline offers great potentials for a diverse range of applications, such as enantioselective chromatography, membrane separations, etc.

Acknowledgement

This work is financially supported by the Engineering and Physical Science Research Council (EPSRC GR/T17953/01).

References

[1] Green MM, Peterson NC, Sato T, Teramoto A, Cook R, Lifson S. Science 1995;268:1860.
[2] Okamoto Y, Yashima E. Angew Chem Int Ed 1998;37:1020.
[3] Peeters E, Christiaans MPT, Schoo HFM, Dekkers HPJM, Meijer EW. J Am Chem Soc 1997;119:9909.
[4] Oda M, Nothofer HG, Gűnter L, Scherf U, Mesker SCJ, Neher D. Adv Mater 2000;12:362.
[5] Langeveld-Voss BMW, Janssen RAJ, Christiaans MPT, Meskers SCJ, Dekkers HPJM, Meijer EW. J Am Chem Soc 1996;118:4908.
[6] Moutet JC, Saintaman E, Tranvan F, Angibeaud P. Adv Mater 1992;4:7.
[7] Huang J, Egan VM, Guo H, Yoon JY, Briseno AL, Rauda IE, et al. Adv Mater 2003;15:1158.
[8] Guo HL, Knobler CM, Kaner RB. Synth Met 1999;101:44.
[9] Bross PA, Schoberl U, Daub J. Adv Mater 1991;3:198.
[10] Reece DA, Kane-Maguire LAP, Wallace GG. Synth Met 2001;119:101.
[11] Majidi MR, Kane-Maguire LAP, Wallace GG. Polymer 1994;35:3113.
[12] Havinga EE, Bouman MM, Meijer EW, Pomp A, Simenon MMJ. Synth Met 1994;66:93.
[13] Pornputtkul Y, Kane-Maguire LAP, Wallace GG. Macromolecules 2006; 39:5604.
[14] Sheridan EM, Breslin CB. Electroanalysis 2005;17:532.

[15] Barisci JN, Innis PC, Kane-Maguire LAP, Norris ID, Wallace GG. Synth Met 1997;84:181.
[16] Yang Y, Wan M. J Mater Chem 2002;12:897.
[17] Tigelaar DM, Lee W, Bates KA, Saprigin A, Prigodin VN, Cao X, et al. Chem Mater 2002;14:1430.
[18] Norris ID, Kane-Maguire LAP, Wallace GG, Mattoso LHC. Aust J Chem 2000;53:89.
[19] Li W, Wang HL. J Am Chem Soc 2004;126:2278.
[20] Li W, Wang HL. Adv Funct Mater 2005;15:1793.
[21] Zhang X, Song W, Harris P, Mitchell J, Bui T, Drake A. Adv Mater 2007;19:1079.
[22] Zhang X, Song W, Harris P, Mitchell J. ChemPhysChem 2007; 8:1766.
[23] Matsushita M, Kuramitz H, Tanaka S. Environ Sci Technol 2005; 39:3805.
[24] Shim YB, Park SM. Synth Met 1989;29:174.
[25] Arvinte T, Bui TTT, Dahab AA, Demeule B, Drake AF, Elhag D, et al. Anal Biochem 2004;332:46.